



Majority-vote model with degree-weighted influence on complex networksMinsuk Kim  and Soon-Hyung Yook **Department of Physics and Research Institute for Basic Sciences, Kyung Hee University, Seoul 130-701, Korea*

(Received 10 September 2020; accepted 6 January 2021; published 2 February 2021)

We study the phase transition of the degree-weighted majority vote (DWMV) model on Erdős-Rényi networks (ERNs) and scale-free networks (SFNs). In this model, a weight parameter α adjusts the level of influence of each node on its connected neighbors. Through the Monte Carlo simulations and the finite-size scaling analysis, we find that the DWMV model on ERNs and SFNs with degree exponents $\lambda > 5$ belongs to the mean-field Ising universality class, regardless of α . On SFNs with $3 < \lambda < 5$ the model belongs to the Ising universality class only when $\alpha = 0$. For $\alpha > 0$ we find that the critical exponents continuously change as α increases from $\alpha = 0$. However, on SFNs with $\lambda < 3$ we find that the model undergoes a continuous transition only for $\alpha = 0$, but the critical exponents significantly deviate from those for the mean-field Ising model. For $\alpha > 0$ on SFNs with $\lambda < 3$ the model is always in the disordered phase.

DOI: [10.1103/PhysRevE.103.022302](https://doi.org/10.1103/PhysRevE.103.022302)**I. INTRODUCTION**

Phase transitions of macroscopic systems have been an important research subject in statistical physics [1]. Spin systems with local interactions such as the Ising model have been fundamental models to study phase transitions and critical phenomena. The spin models also play an important role to understand social collective behaviors such as opinion formation [2]. The models for opinion dynamics based on interacting spin systems show rich interesting phenomena having deep relationships with a wide range of disciplines from physics to sociology and economics [3–5].

The majority-vote (MV) model has been a popular model to investigate the dynamical properties of social phenomena on regular lattices or complex networks [6–8]. The MV model is a nonequilibrium model with up-down symmetry, which shows an order-disorder transition as changing the noise parameter. On low-dimensional regular lattices, the MV model is known to belong to the Ising universality class [9–11]. This agrees with the Grinstein’s conjecture that the nonequilibrium stochastic systems with up-down symmetry belong to the Ising universality class in equilibrium [12].

Recently, the complex network theory has provided a very useful framework for describing many nonregular structures observed in nature [13,14]. Furthermore, models based on such complex networks also have provided theoretical and empirical methods to understand various social phenomena such as information spreading [15], epidemic outbreak [16], propagation of innovation [17], and opinion dynamics [18]. The MV model has been also studied on small-world networks [19,20], random networks [21,22], scale-free networks [23,24], and hyperbolic networks [25]. These studies have shown that the underlying topology affects the transition nature of the MV model and changes the universality class. As an extension of the MV model, the multistate MV model on

regular lattices [26] and complex networks [27–29] are also studied.

The basic assumption of the MV model and its variants is that each agent has the same level of influence on neighboring agents. However, recent studies on social information propagation have revealed that there are superspreaders or superinfluencers on social networks [30]. The superinfluencers have strong ability to affect other people. Thus, they transfer their opinion to more people than normal agents. In order to incorporate the effect of superinfluencers, the MV model with strong opinions [11] was studied on regular lattices. In the MV model with strong opinions, the agents with strong opinion are represented by the superspins. Therefore, the agents with strong opinion denoted by the superspin have larger value of spin than that for normal agents. Numerical simulations showed that the critical noise, at which the order-disorder transition takes place, depends on the concentration of superspins. However, the model belongs to the Ising universality class as the Grinstein’s conjecture.

In social networks, the centrality measures are widely used as a metric for judging the impact of a node on social phenomena [13]. The degree centrality is the simplest centrality among others. Although the degree centrality is the simple one, it is intuitive and illuminating. For example, in citation networks, the highly connected nodes are influential research papers [13]. In epidemiology, the hubs or superspreaders play a big role in disease spreading [16,31]. These examples clearly show that the degree centrality becomes a significant role in spreading dynamics on networks. Furthermore, many centrality measures are positively correlated to each other in general [32–34] including the degree centrality. For example, the random walk centrality of a node is linearly proportional to the degree of the node [35]. Thus, it is natural to assume that the influence of a node is proportional to the degree of the node in opinion dynamics.

In this paper, we introduce a degree-weighted MV (DWMV) model to account for more realistic situations in which the level of influence of a node to its neighborhood is

*syook@khu.ac.kr

proportional to the degree centrality. Thus, a node with a large degree can have more influence on its neighbors than a node with a small degree in the DWMV model. From Monte Carlo (MC) simulations, we find that the DWMV model undergoes an order-disorder transition and the critical noise parameter depends on the underlying topology. In particular, the critical exponents vary continuously as we change the degree-weight parameter when the underlying topology is heterogeneous. This indicates that the universality class of the DWMV model depends not only on the underlying topology but also on the level of influence.

The paper is organized as follows. In Sec. II we define the DWMV model. Section III provides results of the numerical analysis on random networks and scale-free networks. Section IV is the concluding remarks.

II. MODEL

The definition of the DWMV model resembles the original isotropic MV model. In the DWMV model, we assign a spin variable $\sigma_i \in \{-1, +1\}$ to each node i in the network with N nodes. The σ_i represents the opinion of node i . At each step, a node i is randomly selected and determines the degree-weighted majority of the neighboring nodes. The degree-weighted majority of node i , S_i , is defined as

$$S_i = \sum_j a_{ij} \sigma_j [1 + (k_j - 1)\alpha], \quad (1)$$

where k_j is the degree of node j and $\alpha \in [0, 1]$ is the degree-weight parameter, which adjusts the level of additional influence. a_{ij} is an element of the adjacency matrix, which is defined as $a_{ij} = 1$ if the nodes i and j are connected and $a_{ij} = 0$ otherwise. Then the spin of the selected node i is flipped with the probability

$$w(\sigma_i) = \frac{1}{2} [1 - (1 - 2q)\sigma_i \text{sgn}(S_i)], \quad (2)$$

where $\text{sgn}(x) = +1, 0, -1$ in case $x > 0, x = 0,$ and $x < 0$, respectively. When $\text{sgn}(S_i) = 0$, $\sigma_i = \pm 1$ is randomly assigned. Therefore, the selected node follows the degree-weighted majority state with the probability $1 - q$, or adopts the opposite state with the probability q . The probability q is called the noise parameter, which plays a similar role of temperature in the equilibrium spin models. For $\alpha = 0$, the DWMV model recovers the original isotropic MV model. However, when $\alpha > 0$, the opinion of a node can be determined only by a single neighbor with a large k due to the degree-weighted influence.

To investigate the critical behavior of the model, we measure the magnetization, $M(q, N)$, the susceptibility, $\chi(q, N)$, and the Binder's fourth-order cumulant, $U(q, N)$. These quantities are defined as

$$M(q, N) = \langle \langle m \rangle_t \rangle_c, \quad (3)$$

$$\chi(q, N) = N \left[\langle \langle m^2 \rangle_t \rangle_c - \langle m \rangle_t^2 \right], \quad (4)$$

$$U(q, N) = 1 - \left\langle \frac{\langle m^4 \rangle_t}{3 \langle m^2 \rangle_t^2} \right\rangle_c, \quad (5)$$

where $m = |\sum_{i=0}^N \sigma_i / N|$. $\langle \dots \rangle_t$ and $\langle \dots \rangle_c$ denote the temporal averages measured in the steady state and the configurational averages, respectively.

For each value of α we perform MC simulations on networks with $N = 10000, 20000, 40000, 80000, 160000$ for ERNs and SFNs with $\lambda > 3$. For SFNs with $\lambda < 3$, we use $N = 10000 \sim 320000$ due to the strong finite-size effect. In our simulations, time is measured in Monte Carlo steps (MCSs). At each unit MCS there are N trials of spin flipping, i.e., each node tries to update its state once on average. The completely ordered configuration in which all nodes have the same value of spin is used as an initial condition. Since we find that the DWMV model is in the steady state when $t = 10^4$ MCSs for $N = 320000$ on ERNs and SFNs, we discard the initial 5×10^4 MCSs in the following simulations. The time averages are obtained from the next 10^4 MCSs. For all parameter sets (α, q) , the configurational averages are obtained from at least 300 network realizations. In the critical regime, at least 1000 network realizations are used to obtain the configurational averages due to large fluctuations.

Two different types of underlying networks, Erdős-Rényi networks (ERNs) and scale-free networks (SFNs) are used [13]. ERNs are characterized by a Poisson degree distribution $p(k) = \langle k \rangle^k e^{-\langle k \rangle} / k!$. On the other hand, SFNs have a power-law degree distribution $p(k) \sim k^{-\lambda}$, where λ is the degree exponent. To generate ERNs and SFNs with various λ , we use the static model [36]. Thus, the networks have the natural degree cutoff, k_{\max} , which scales as $k_{\max} \sim N^{-1/(1-\lambda)}$ [14]. In the following numerical simulations, we set the mean degree $\langle k \rangle = 10$ for both networks.

III. RESULTS

A. Erdős-Rényi networks

In Figs. 1(a) and 1(b) we show the measured $U(q, N)$ for $\alpha = 0$ and $\alpha = 1$ on ERNs with $N = 10000 \sim 160000$. The critical noise, q_c , for a given value of α is estimated as the point at which the curves for different N intersect each other. From the data, we obtain $q_c = 0.3004 \pm 0.0004$ for $\alpha = 0$ and $q_c = 0.3008 \pm 0.0004$ for $\alpha = 1$. We also measure q_c 's for other values of α using $U(q, N)$. From the obtained q_c 's we plot the phase diagram of the DWMV model in the inset of Fig. 1(b). As shown in the phase diagram, the values of q_c for each α are identical within the estimated errors for $0 \leq \alpha \leq 1$. We also measure $M(q, N)$ and $\chi(q, N)$ on ERNs for various values of α . To obtain the critical exponents we use the finite-size scaling ansatz [1,37]

$$M(q, N) \sim N^{-\beta/\bar{\nu}} \tilde{M}(\epsilon N^{1/\bar{\nu}}), \quad (6)$$

$$\chi(q, N) \sim N^{\gamma/\bar{\nu}} \tilde{\chi}(\epsilon N^{1/\bar{\nu}}), \quad (7)$$

$$U(q, N) \sim \tilde{U}(\epsilon N^{1/\bar{\nu}}), \quad (8)$$

where $\epsilon = q - q_c$ and \tilde{M} , $\tilde{\chi}$, and \tilde{U} are universal scaling functions. β , γ , and $\bar{\nu}$ are the critical exponents for the order parameter, the susceptibility, and the correlation volume, respectively. The correlation volume exponent is defined as $\bar{\nu} = d_u \nu$, where d_u is the upper critical dimension and ν is the correlation length exponent [38]. $\bar{\nu}$ can be obtained from the

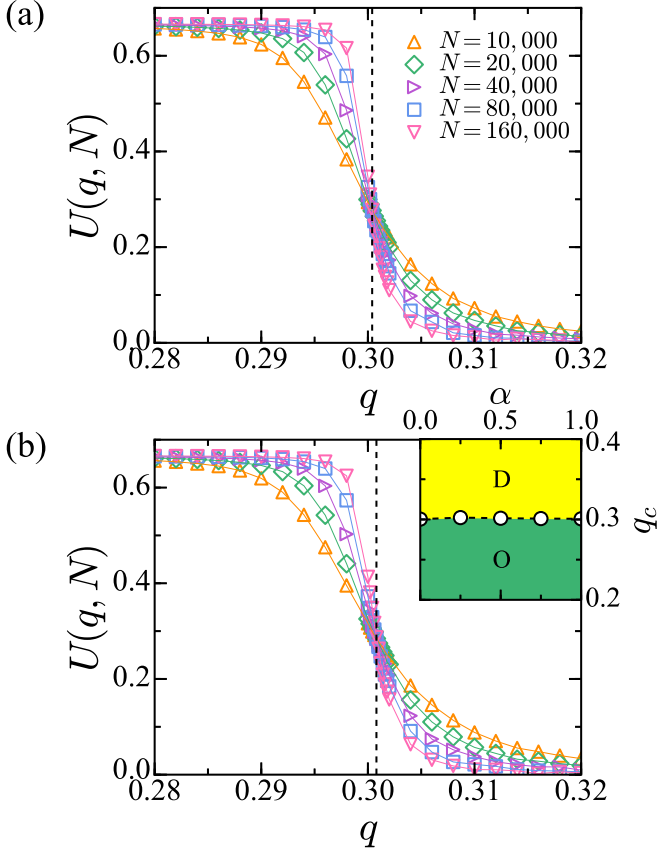


FIG. 1. Plot of $U(q, N)$ on ERNs with various N for (a) $\alpha = 0$ and (b) $\alpha = 1$. The vertical lines represent the estimated critical noise, (a) $q_c = 0.3004$ and (b) $q_c = 0.3008$. Inset: phase diagram of DWMV model on ERNs. “O” and “D” represent the ordered phase and the disordered phase, respectively.

scaling relation

$$q_c(N) = q_c + bN^{-1/\bar{\nu}}, \quad (9)$$

where b is a constant and $q_c(N)$ is the value of q at which $\chi(q, N)$ has the maximum value. Alternatively, $\bar{\nu}$ is also obtained from the derivative of $U(q, N)$ [25],

$$|dU(q, N)/dq| \sim N^{1/\bar{\nu}} \tilde{U}'(\epsilon N^{1/\bar{\nu}}). \quad (10)$$

By using Eqs. (6)–(10), we obtain $1/\bar{\nu} = 0.5$, $\beta/\bar{\nu} = 0.25$, and $\gamma/\bar{\nu} = 0.5$ on ERNs, which are exactly the same with those for the mean-field Ising model [1]. In Fig. 2, we show that $M(q, N)$ and $\chi(q, N)$ on ERNs with various N for $\alpha = 1$ collapse into the corresponding universal scaling functions with the obtained exponents. For other values of $\alpha \in [0, 1]$ we obtain the same exponents (which is not shown). These results clearly show that the DWMV model on ERNs belongs to the Ising universality class, regardless of α .

B. Scale-free networks with $\lambda > 5$

Since SFNs with $\lambda \rightarrow \infty$ is generally regarded as an exponential random network, many physical systems on SFNs with large λ show the same behavior as on ERNs. For example, the Ising model on SFNs with $\lambda > 5$ shows the mean-field behavior [38,39]. On the other hand, when $\lambda < 5$,

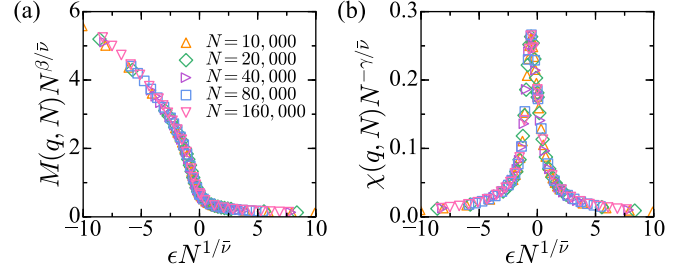


FIG. 2. Data collapse for (a) $M(q, N)$ and (b) $\chi(q, N)$ when $\alpha = 1$ on ERNs with the critical exponents $1/\bar{\nu} = 0.5$, $\beta/\bar{\nu} = 0.25$, and $\gamma/\bar{\nu} = 0.5$.

a nontraditional singularity emerges. Similarly, the DWMV model shows a crossover from a mean-field to a nontraditional behavior at $\lambda \simeq 5$. The data in Fig. 3 shows the scaling collapse for $\chi(q, N)$ and $M(q, N)$ when $\lambda = 5.2$ and $\alpha = 1$ using $q_c = 0.2948 \pm 0.0004$, $1/\bar{\nu} = 0.47 \pm 0.04$, $\gamma/\bar{\nu} = 0.57 \pm 0.03$, and $\beta/\bar{\nu} = 0.21 \pm 0.04$. These values of exponents are quite close to those for the mean-field Ising model. Furthermore, we find that all the critical exponents do not depend on α for $\lambda > 5$ as in the case on ERNs. This shows that the DWMV model on SFNs with $\lambda > 5$ also belongs to the Ising universality class, regardless of the value of α . This implies that there is no superinfluencer or opinion leader in the DWMV model on homogeneous networks if the level of the influence is proportional to the degree centrality.

C. Scale-free networks with $3 < \lambda < 5$

Unlike on ERNs or SFNs with $\lambda > 5$, the DWMV model on SFNs with $\lambda < 5$ does not belong to the Ising universality class when $\alpha > 0$. Due to the heterogeneity of degree in SFNs with $3 < \lambda < 5$, q_c is significantly affected by α even for a very small value of α . As an example, we show the measured $U(q, N)$ on SFNs with $\lambda = 3.7$ for $\alpha = 0.01$ in Fig. 4(a). From the data we obtain $q_c = 0.3221 \pm 0.0004$. Using $U(q, N)$ for other values of α , we also estimate q_c 's for each α on SFNs with $\lambda = 3.7$. The obtained q_c decreases

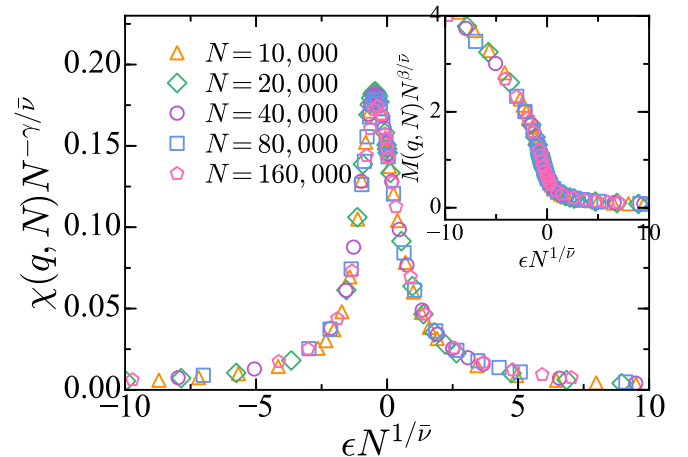


FIG. 3. Data collapse for $\chi(q, N)$ on SFNs with $\lambda = 5.2$, $q_c = 0.2948$, $1/\bar{\nu} = 0.47$, $\gamma/\bar{\nu} = 0.57$ when $\alpha = 1$. Inset: Data collapse for $M(q, N)$ with $\beta/\bar{\nu} = 0.21$.

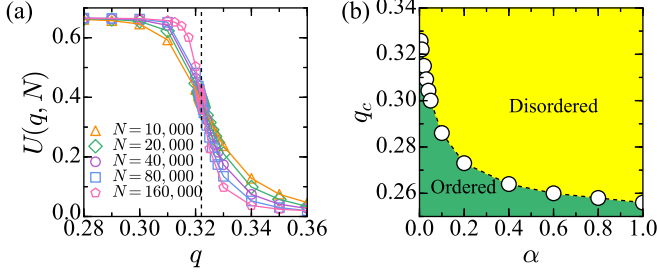


FIG. 4. (a) Plot of $U(q, N)$ on SFNs with $\lambda = 3.7$ for $\alpha = 0.01$ and $N = 10000 \sim 160000$. Vertical line represents the intersection of $U(q, N)$'s, from which $q_c = 0.3221$ is estimated. (b) Phase diagram for SFNs with $\lambda = 3.7$.

monotonically as α increases as shown in Fig. 4(b). On SFNs with $3 < \lambda < 5$ if a node is connected to a node of large k , then the state of the node is substantially affected by the state of the node of the large k when α becomes large. This means that if the state of the large k node is changed then the neighboring nodes also follow the decision of the large k node. Thus, the node of large k easily becomes the super-influencer when α is large. If there are more than one superinfluencer with different opinions, then there can be a competition between them. Due to the competition, the disordered phase is more favorable than the ordered phase even for relatively small q as α increases. As a result, q_c decreases as α increases. Similar behavior was observed in the strong opinion MV model [11] and the zero-temperature Glauber dynamics on SFNs [40]. In order to obtain $1/\bar{\nu}$, we use Eq. (9). The data in the inset of Fig. 5 shows $q_c - q_c(N)$ for SFNs with $\lambda = 3.7$

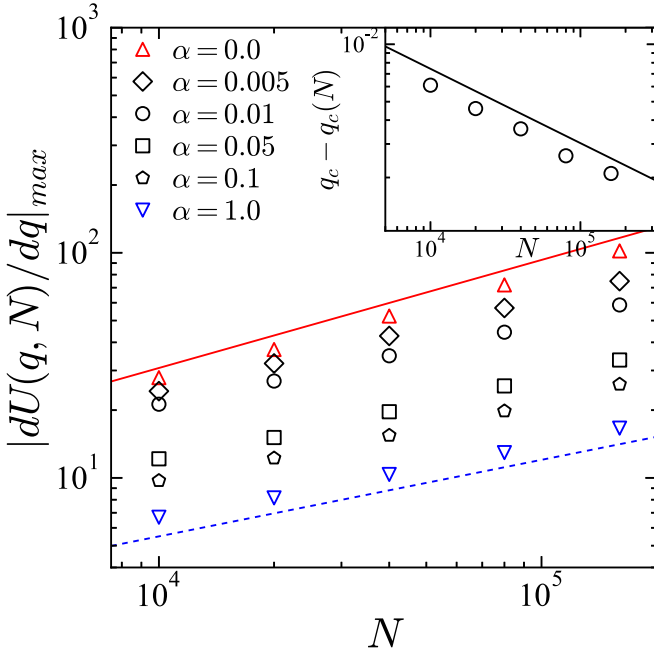


FIG. 5. Plot of maximum of $|dU(q, N)/dq|$ on SFNs ($\lambda = 3.7$) for various α 's. The solid line corresponds to $|dU(q, N)/dq| \sim N^{0.48}$ and dashed line denotes $|dU(q, N)/dq| \sim N^{0.34}$. Inset: Plot of $q_c - q_c(N)$ against N for $\alpha = 0.01$. The solid line represents the relation $q_c - q_c(N) \sim N^{-0.39}$.

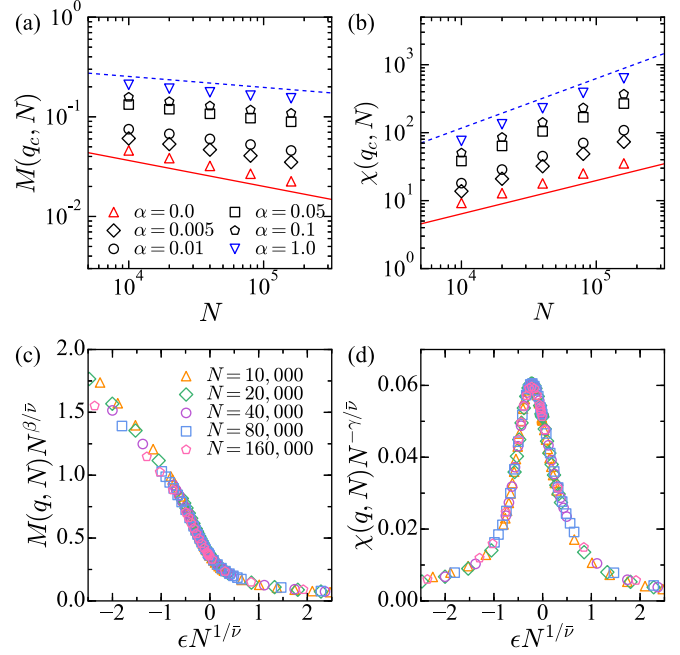


FIG. 6. Plot of (a) $M(q_c, N)$ and (b) $\chi(q_c, N)$ on SFNs with $\lambda = 3.7$ for various values α . (a) The solid line represents $M \sim N^{-0.26}$ and the dashed line denotes $M \sim N^{-0.11}$. (b) The solid line corresponds to $\chi \sim N^{0.49}$ and the dashed line represents $\chi \sim N^{0.74}$. Data collapse for (c) $M(q, N)$ and (d) $\chi(q, N)$ with $1/\bar{\nu} = 0.39$, $\beta/\bar{\nu} = 0.17$, and $\gamma/\bar{\nu} = 0.64$ when $\alpha = 0.01$.

and $\alpha = 0.01$ as an example. From the best fit of the data to Eq. (9) we obtain $1/\bar{\nu} = 0.39 \pm 0.03$. However, when α is large, $q_c - q_c(N)$ becomes very small, and it is hard to obtain the accurate value of $1/\bar{\nu}$ using Eq. (9). Thus for a better estimation of $1/\bar{\nu}$ we use Eq. (10). The data in Fig. 5 shows the maximum of $|dU(q, N)/dq|$, $|dU(q, N)/dq|_{\max}$, as a function of N for various values of α [25]. From the data of $|dU(q, N)/dq|_{\max}$ for $\alpha = 0.01$, we obtain $1/\bar{\nu} = 0.39 \pm 0.03$, which agrees with $1/\bar{\nu}$ estimated from Eq. (9). When $\alpha = 0$ we obtain $1/\bar{\nu} = 0.48 \pm 0.02$ using Eq. (10). This value of $1/\bar{\nu}$ is identical with that of the mean-field Ising model within the estimated error. As α increases, $1/\bar{\nu}$ decreases continuously, and we obtain $1/\bar{\nu} = 0.34 \pm 0.07$ for $\alpha = 1$. In Fig. 6(a) $M(q, N)$ at q_c on SFNs with $\lambda = 3.7$ for various values of α is displayed. For $\alpha = 0$ we obtain $\beta/\bar{\nu} = 0.26 \pm 0.03$ using the relation $M(q_c, N) \sim N^{-\beta/\bar{\nu}}$. The obtained value of $\beta/\bar{\nu}$ is identical with that of the mean-field Ising model within the estimated error. However, if $\alpha \neq 0$ then $\beta/\bar{\nu}$ significantly deviates from $\beta/\bar{\nu} = 0.25$, i.e., as α increases we find that $\beta/\bar{\nu}$ continuously decreases and reaches $\beta/\bar{\nu} = 0.11 \pm 0.03$ for $\alpha = 1$. We find the similar behavior for $\chi(q, N)$. For $\alpha = 0$ we obtain $\gamma/\bar{\nu} = 0.49 \pm 0.04$ from the relation $\chi(q_c, N) \sim N^{\gamma/\bar{\nu}}$, which is the same with that of the mean-field Ising model within the estimated error. As α increases, we find that $\gamma/\bar{\nu}$ continuously increases and reaches $\gamma/\bar{\nu} = 0.74 \pm 0.06$ for $\alpha = 1$ [see Fig. 6(b)]. In Figs. 6(c) and 6(d) we show the scaling collapse for $M(q, N)$ and $\chi(q, N)$ with the obtained exponents for $\lambda = 3.7$ and $\alpha = 0.01$, as an example. Furthermore, we find that the obtained

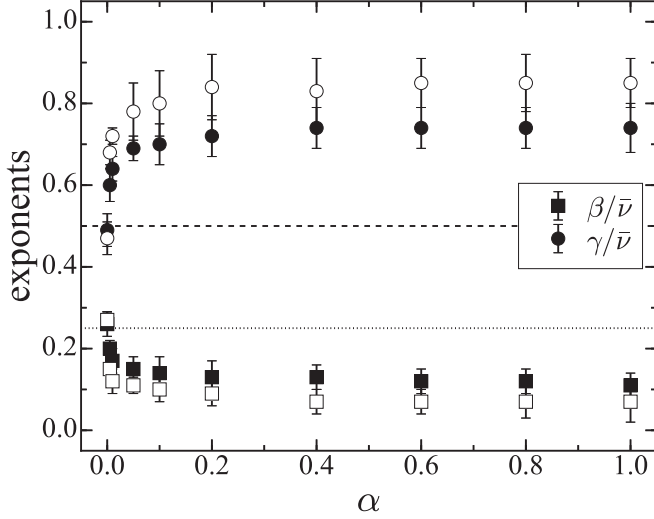


FIG. 7. Plot of β/\bar{v} (squares) and γ/\bar{v} (circles) against α on SFNs with $\lambda = 3.7$ (filled symbols) and $\lambda = 3.4$ (open symbols). The horizontal lines denote the mean-field Ising exponents, $\beta/\bar{v} = 0.25$ (dotted line), and $\gamma/\bar{v} = 0.5$ (dashed line)

β , γ , and \bar{v} , satisfy the hyperscaling relation [1,29]

$$2\beta/\bar{v} + \gamma/\bar{v} = 1, \quad (11)$$

for all values of α .

We also measure $M(q, N)$ and $\chi(q, N)$ for other values of λ ($3 < \lambda < 5$), and find that they show the similar behavior as on SFNs with $\lambda = 3.7$. For example, we display the measured β/\bar{v} and γ/\bar{v} as a function of α for both $\lambda = 3.4$ and $\lambda = 3.7$ in Fig. 7. The obtained exponents satisfy the hyperscaling relation, Eq. (11), and clearly shows that the critical exponents continuously approaches to those for the mean-field Ising model, $\beta/\bar{v} = 0.25$, and $\gamma/\bar{v} = 0.5$, as $\alpha \rightarrow 0$. In addition, these critical exponents also depend on λ as shown in Fig. 7.

From these results, we find that the DWMV model belongs to the Ising universality class when $\alpha = 0$, which corresponds to the isotropic MV model. However, if the degree-dependent weight is introduced ($\alpha > 0$) then the model does not belong to the Ising universality class. Furthermore, the critical exponents of the DWMV model on SFNs with $3 < \lambda < 5$ continuously change from those of the mean-field Ising model as α increase from $\alpha = 0$.

D. Scale-free networks with $\lambda < 3$

The phase transition of the isotropic MV model on SFNs with $\lambda < 3$ is rarely studied, and typically focused on the dependency of q_c on the underlying topology [24]. The phase transition of the DWMV model on SFNs with $\lambda < 3$ is subtle. For $\lambda < 3$, the critical behavior of the DWMV model is significantly affected by hubs. For $\alpha = 0$, we obtain $q_c = 0.381 \pm 0.004$, $1/\bar{v} = 0.31 \pm 0.04$, $\beta/\bar{v} = 0.25 \pm 0.05$, and $\gamma/\bar{v} = 0.51 \pm 0.04$ from the finite-size scaling [for example, see the insets of Figs. 8(a) and 8(b)]. In Ref. [24], $1/\bar{v}$ for the isotropic MV model is also measured through MC simulations. By using the interpolation, we expect that $1/\bar{v} \simeq 0.22$ from the data provided by Chen *et al.* in Ref. [24]. The obtained value of $1/\bar{v}$ in our simulations seems to be slightly

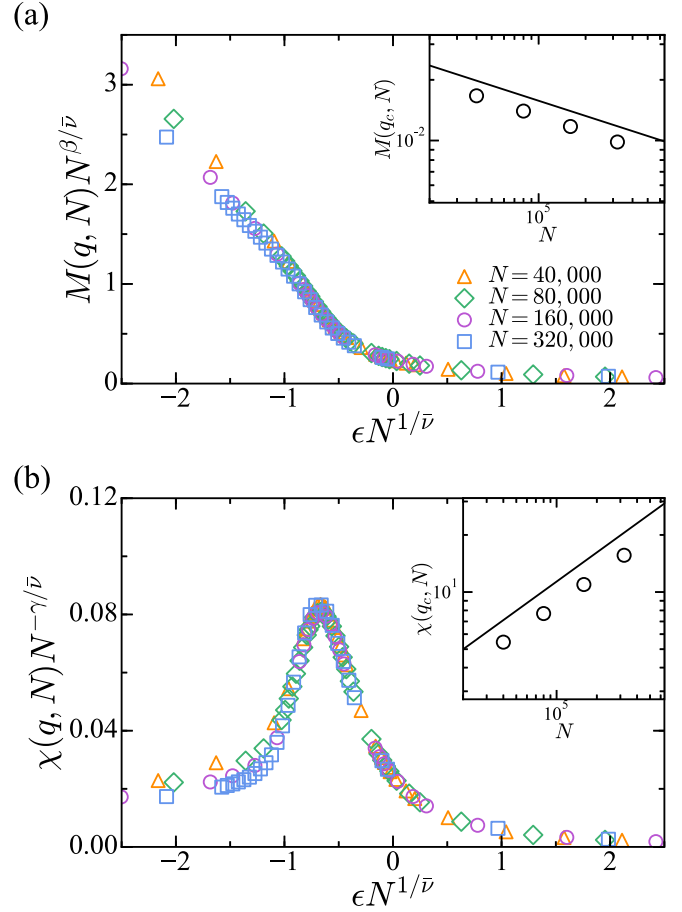


FIG. 8. Data collapse for (a) $M(q, N)$ and (b) $\chi(q, N)$ on SFNs with $\lambda = 2.7$ and $\alpha = 0$. We use $q_c = 0.381$, $1/\bar{v} = 0.31$, $\beta/\bar{v} = 0.25$, and $\gamma/\bar{v} = 0.51$. Insets: Plot of (a) $M(q_c, N)$ and (b) $\chi(q_c, N)$ against N . The lines denote (a) $M(q_c, N) \sim N^{-0.25}$ and (b) $\chi(q_c, N) \sim N^{0.51}$.

larger than that expected by Chen *et al.* [41]. Using the obtained exponents we find that $M(q, N)$ and $\chi(q, N)$ collapse into the universal scaling functions as shown in Figs. 8(a) and 8(b). In contrast to the case of $\alpha = 0$, when $\alpha > 0$ the obtained $M(q, N)$ and $\chi(q, N)$ do not satisfy the finite-scaling ansatz, Eqs. (6)–(10). In Fig. 9(a) we display $M(q, N)$ for $\alpha = 0.001$ measured on SFNs with $\lambda = 2.7$. The data shows that there seems to be a phase transition from the ordered phase to the disordered one as q increases. However, we find that $M(q, N)$ systematically decreases as N increases in the ordered regime, regardless of the values of $\alpha (> 0)$ [see the inset of Fig. 9(a)]. In order to find the asymptotic behavior of $M(q, N)$ we define the difference in the magnetization as $\Delta_N = M(q, N/2) - M(q, N)$. The data in Fig. 9(b) shows the obtained Δ_N for $\alpha = 0.001$ and $q = 0.02$ in the log-linear plot. The data shows that Δ_N grows logarithmically as N increases. This means that $M(q, N)$ logarithmically vanishes as N increases. Therefore, we expect that $M(q, N) \rightarrow 0$ in the limit $N \rightarrow \infty$. However, due to the slow logarithmic growth of Δ_N , we cannot observe the asymptotic value $M(q, \infty) = 0$ through the finite-size simulations. When we increase α , we find slightly different behavior of Δ_N [see, for example, Fig. 9(c)]. As α increases, we find that Δ_N seems to decrease.

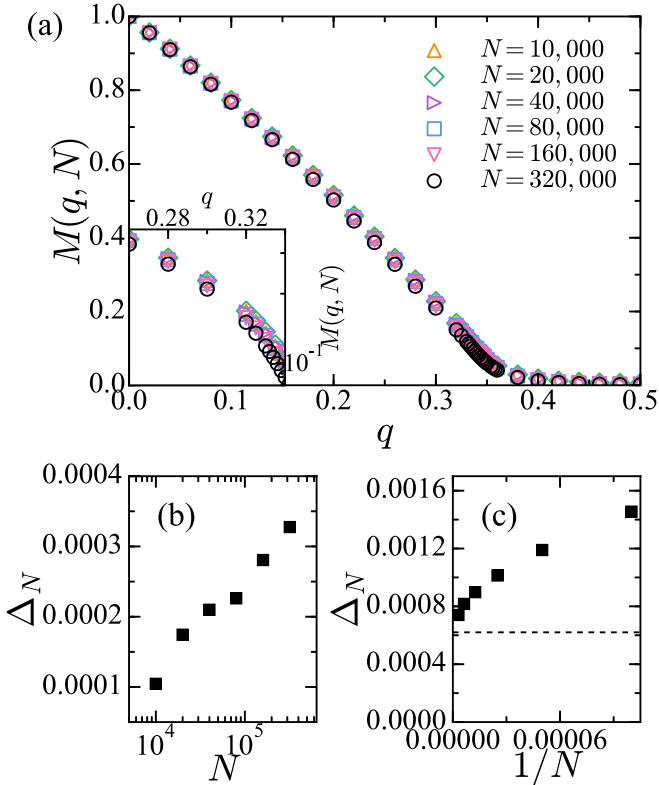


FIG. 9. (a) $M(q, N)$ on SFNs with $\lambda = 2.7$ when $\alpha = 0.001$. (inset) linear-log plot of (a) for $q \in [0.26, 0.34]$. (b) Plot of Δ_N against N for $\alpha = 0.001$ and $q = 0.02$. (c) Plot of Δ_N against $1/N$ for $\alpha = 0.5$ and $q = 0.02$. Dashed line: $y \approx 0.0006$.

However, from an extrapolation of the data, we expect that $\Delta_N \rightarrow 0.0006 (>0)$ in the limit $N \rightarrow \infty$. This also indicates that $M(q, N)$ is expected to be vanished in the thermodynamic limit.

IV. SUMMARY

In this study, we investigate the phase transition of the DWMV model on complex networks. The state of each node is determined by the degree-weighted majority of the connected neighbors with the probability $1 - q$, while it takes the minority state with the probability q . The weight parameter α adjusts the level of the degree-weighted influence on each node. By performing extensive Monte Carlo simulations, we find that the DWMV model undergoes an order-disorder transition on ERNs and SFNs with $\lambda > 3$. Furthermore, through the finite-scaling analysis on ERNs and SFNs with $\lambda > 5$, we find that the model belongs to the mean-field Ising universality class, regardless of the value of α . This result agrees with Grinstein's conjecture [12] as in the MV model with strong opinion [11]. On the other hand, on SFNs with $3 < \lambda < 5$, the model belongs to the mean-field Ising universality class only when $\alpha = 0$. For $\alpha > 0$, we find that q_c and the critical exponents continuously change as α increases.

On SFNs with $\lambda < 3$ the transition is subtle. For $\alpha = 0$, we find that the DWMV model undergoes a phase transition. However, the obtained exponents significantly deviate from those for the mean-field Ising model. Furthermore, even though we observe that the $M(q, N) > 0$ for small q and $\alpha > 0$ on finite-size networks with $\lambda < 3$, by measuring Δ_N we find that $M(q, N)$ decreases logarithmically as N increases. Thus, the ordered phase should disappear in the thermodynamic limit for $\alpha > 0$ on SFNs with $\lambda < 3$. The results also show that if the interaction topology between individuals can be approximated by SFNs with $\lambda < 5$, the one who has a large degree can play a significant role in opinion formation.

ACKNOWLEDGMENT

This research was supported by Basic Science Research Program through the National Research Foundation of Korea (NRF) funded by the Ministry of Education (Republic of Korea) (Grant No. NRF-2019R1F1A1058549).

- [1] H. E. Stanley, *Introduction to Phase Transitions and Critical Phenomena* (Oxford University Press, Oxford, 1971).
- [2] T. M. Liggett, *Stochastic Interacting Systems: Contact, Voter, and Exclusion Processes* (Springer-Verlag, New York, 1999).
- [3] Y. Kim, H.-J. Kim, and S.-H. Yook, *Phys. Rev. E* **78**, 036115 (2008).
- [4] C. Castellano, S. Fortunato, and V. Loreto, *Rev. Mod. Phys.* **81**, 591 (2009).
- [5] A. Vespignani, *Nature Phys.* **8**, 32 (2012).
- [6] T. Tome, M. J. de Oliveira, and M. A. Santos, *J. Phys. A: Math. Gen.* **24**, 3677 (1991).
- [7] M. J. de Oliveira, *J. Stat. Phys.* **66**, 273 (1992).
- [8] H. Zhou and R. Lipowsky, *Proc. Nat. Acad. Sci.* **102**, 10052 (2005).
- [9] A. L. Acuña-Lara and F. Sastre, *Phys. Rev. E* **86**, 041123 (2012).
- [10] U. Yu, *Phys. Rev. E* **95**, 012101 (2017).
- [11] A. L. M. Vilela and H. E. Stanley, *Sci. Rep.* **8**, 8709 (2018).
- [12] G. Grinstein, C. Jayaprakash, and Y. He, *Phys. Rev. Lett.* **55**, 2527 (1985).
- [13] M. E. J. Newman, *Networks*, 2nd ed. (Oxford University Press, Oxford, 2018).
- [14] A.-L. Barabási, *Network Science* (Cambridge University Press, Cambridge, 2016).
- [15] S.-H. Yook and Y. Kim, *Phys. Rev. E* **101**, 012312 (2020).
- [16] R. Pastor-Satorras and A. Vespignani, *Phys. Rev. Lett.* **86**, 3200 (2001).
- [17] Y. Kim, B. Han, and S.-H. Yook, *Phys. Rev. E* **82**, 046110 (2010).
- [18] V. Sood and S. Redner, *Phys. Rev. Lett.* **94**, 178701 (2005).
- [19] P. R. A. Campos, V. M. de Oliveira, and F. G. Brady Moreira, *Phys. Rev. E* **67**, 026104 (2003).
- [20] T. E. Stone and S. R. McKay, *Physica A* **419**, 437 (2015).
- [21] L. F. C. Pereira and F. G. Brady Moreira, *Phys. Rev. E* **71**, 016123 (2005).
- [22] F. W. S. Lima, A. O. Sousa, and M. A. Sumuor, *Physica A* **387**, 3503 (2008).

- [23] F. W. S. Lima, *Int. J. Mod. Phys. C* **17**, 1257 (2006).
- [24] H. Chen, C. Shen, G. He, H. Zhang, and Z. Hou, *Phys. Rev. E* **91**, 022816 (2015).
- [25] Z.-X. Wu and P. Holme, *Phys. Rev. E* **81**, 011133 (2010).
- [26] A. Brunstein and T. Tomé, *Phys. Rev. E* **60**, 3666 (1999).
- [27] G. Li, H. Chen, F. Huang, and C. Shen, *J. Stat. Mech.* (2016) 073403.
- [28] H. Chen and G. Li, *Phys. Rev. E* **97**, 062304 (2018).
- [29] A. L. M. Vilela, B. J. Zubillaga, C. Wang, M. Wang, R. Du, and H. E. Stanley, *Sci. Rep.* **10**, 8255 (2020).
- [30] J.-X. Zhang, D.-B. Chen, Q. Dong, and Z.-D. Zhao, *Sci. Rep.* **6**, 27823 (2016).
- [31] A. L. Lloyd and R. M. May, *Science* **292**, 1316 (2001).
- [32] M. E. J. Newman, *Soc. Networks* **27**, 39 (2005).
- [33] S. Lee, S.-H. Yook, and Y. Kim, *Eur. Phys. J. B* **68**, 277 (2009).
- [34] S. Oldham, B. Fulcher, L. Parkes, A. Arnatkevičiūtė, C. Suo, and A. Fornito, *PLoS ONE* **14**, e0220061 (2019).
- [35] J. D. Noh and H. Rieger, *Phys. Rev. Lett.* **92**, 118701 (2004).
- [36] K.-I. Goh, B. Kahng, and D. Kim, *Phys. Rev. Lett.* **87**, 278701 (2001).
- [37] V. Privman, *Finite-Size Scaling and Numerical Simulation of Statistical Systems* (World Scientific, Singapore, 1990).
- [38] H. Hong, M. Ha, and H. Park, *Phys. Rev. Lett.* **98**, 258701 (2007).
- [39] A. V. Goltsev, S. N. Dorogovtsev, and J. F. F. Mendes, *Phys. Rev. E* **67**, 026123 (2003).
- [40] C. Castellano and R. Pastor-Satorras, *J. Stat. Mech.* (2006) P05001.
- [41] On SFNs with $\lambda < 3$ measuring the critical point and exponents are not trivial for many physical systems due to the strong finite-size effect. In Ref. [24], the largest size of networks is $N = 10000$. However, $N = 40000$ is the smallest size of underlying networks in our simulations. Thus, we expect that the discrepancy of the value of $1/\bar{v}$ is originated from the difference in the size of networks for MC simulations.